Supplemental Information

Supplemental figure 1. Lists of genes whose expression was decreased (A) or increased (B) in the liver of *Ire1α*-null (*Ire1α*$^{Hepfe/-}$) mice, compared to the control (*Ire1α*$^{Hepfe/+}$) mice, in the absence of TM treatment. The normalized average expression values were based on the microarray analysis. The genes whose expression was changed at least 1.5-folds were listed ($p<0.05$).

Supplemental figure 2. (**A**) Levels of intracellular triglycerides in liver tissues of *Ire1α*-null (*Ire1α*$^{Hepfe/-}$) and control (*Ire1α*$^{Hepfe/+}$) mice after intraperitoneal injection of TM (2μg/gram body weight) or vehicle (150 μM dextrose) for 24 hours. The mice were fasted for 8 hours before euthanized for collecting samples. Each bar denotes the mean ± SEM (n=6 mice per group). * P<0.05. (**B-C**) Levels of liver cellular phospholipids, including phosphatidylethanolamine (PtdEtn), phosphatidylcholine (PtdCho), and sphingomyelin (SM), in the *Ire1α*$^{Hepfe/-}$ and *Ire1α*$^{Hepfe/+}$ mice after intraperitoneal injection with the vehicle or TM for 8 hours. Each bar denotes the mean ± SEM (n=3 mice per group). * P<0.05. (**D**) Western blot analysis of phoshocholine cytidylyltransferase alpha (CCTα) protein in the *Ire1α*$^{Hepfe/-}$ and *Ire1α*$^{Hepfe/+}$ mice after intraperitoneal injection with the vehicle or TM for 8 hours. Levels of α-tubulin were determined as internal controls. The CCTα antibody can detect an unspecific band below CCTα band with mouse liver tissue samples.

Supplemental figure 3. Quantitative real-time PCR analysis of the mouse *Pparγ2* gene expression in the liver or fat tissue of mice after high-fat feeding or in the liver of mice after TM treatment. (**A**) Threshold cycle numbers of quantitative real-time PCR analysis for the *Pparγ2* mRNA expression in the white fat and liver tissues of mice after the high-fat diet or in the liver tissue of mice after TM treatment. C57BL/6J mice of 8-weeks old were fed with a high-fat diet (42%

fat, TD 88137, Harland Teklad) for 2 months. Total RNA was isolated from the white adipose or liver tissue for the quantitative real-time PCR analysis. The Ire1α-null (*Ire1α*$^{Hepfe/-}$) and control (*Ire1α*$^{Hepfe/+}$) mice were challenged with TM (2μg/gram body weight) or vehicle (150 μM dextrose) for 8 hrs. Total RNA was isolated from the liver tissue for the quantitative real-time PCR analysis. The real-time PCR primer sequences for amplifying the *Pparγ2* mRNA are 5'-TCTGGGAGATTCTCCTGTTGA-3' and 5'-GGTGGGCCAGAATGGCATCT-3'. (**B**) The relative *Pparγ2* mRNA levels (fold changes) in the white adipose tissue (WAT) and liver of mice after the high-fat diet for 2 months or in the liver of mice after TM treatment for 8 hrs. The fold changes of the *Pparγ2* mRNA levels were calculated based on the real-time PCR analysis (n=5 for high-fat-fed mice group, and n=3 for TM-treated mice group).

Supplemental figure 4. Quantitative real-time RT-PCR analysis for fold changes in expression of the *Acox1*, *Cpt1a*, *Cyp4a10*, *Fabp1*, *MTTP*, *Fatp2*, *Fsp27*, *aP2*, and *Fat/Cd36* mRNAs in the livers of the *Ire1α*$^{Hepfe/-}$ and *Ire1α*$^{Hepfe/+}$ mice. Total RNAs from the livers of mice challenged with TM (2 μg/gram body weight) or vehicle for 8 hours were subjected to quantitative real-time RT-PCR analysis. Expression values were normalized to the *β-actin* mRNA levels. Fold changes of mRNA levels were shown by comparison to the expression level of mRNA in one of the control (*Ire1α*$^{Hepfe/+}$) mice. Each bar denotes the mean ± SEM (n=6 mice per group). * P<0.05; ** P<0.01.

Supplemental figure 5. Quantitative real-time RT-PCR analysis for fold changes in expression of the *Pparα*, *Pparδ*, *Pgc-1α*, *Pgc-1β*, *Fasn*, and *Srebp-1c* mRNAs in the livers of the *Ire1α*$^{Hepfe/-}$ and *Ire1α*$^{Hepfe/+}$ mice. Total RNAs from the livers of mice challenged with TM (2 μg/gram body weight) or vehicle for 8 hours were subjected to quantitative real-time RT-PCR analysis. Expression values were normalized to the *β-actin* mRNA levels. Fold changes of mRNA levels were shown by

comparison to the expression level of mRNA in one of the control (*Ire1α*$^{Hepfe/+}$) mice. Each bar denotes the mean ± SEM (n=6 mice per group). * P<0.05.

Supplemental figure 6. Mice with hepatocyte-specific *Ire1α* deletion exhibit increased apoptosis in response to Bortezomib treatment. *Ire1α*-null *(Ire1α*$^{Hepfe/-}$) and control (*Ire1α*$^{Hepfe/+}$) mice were injected with Bortezomib (1μg/gram body weight) into the tail vein. At 36 hours after injection, the mice were fasted for 8 hours prior to euthanasia and collection of liver tissue samples. (**A**) Immunofluorescent TUNEL staining of liver tissue sections for analysis of DNA fragmentation (magnification: 400×). The apoptotic cells exhibited green fluorescence. The cells were also stained with propidium iodide (PI), to identify all cells by strong red cytoplasmic fluorescence. (**B**) The percentages of TUNEL-positive cells (green fluorescence) determined by calculating the number of TUNEL-positive cells divided by the number of PI-positive cells (red fluorescence) from five fields of each slide. ** *P*<0.01.

Supplemental figure 7. *Ire1α*-null mice displayed profound hepatic steatosis after partial hepatectomy. *Ire1α*-null *(Ire1α*$^{Hepfe/-}$) and control (*Ire1α*$^{Hepfe/+}$) mice of 3-months old were subjected to 2/3 partial hepatectomy as previously described (Mitchell & Willenbring, 2008). Briefly, the mice were anesthetized with 2% isoflurane and 2 liters/min oxygen flow for 25g body weight, followed by removal of 2/3 liver lobes. At 60 hrs after the hepatectomy surgery, the liver tissues were collected for lipid droplet staining and measurement of hepatic triglycerides. (**A**) Liver tissue sections from the *Ire1α*-null (*Ire1α*$^{Hepfe/-}$) and control (*Ire1α*$^{Hepfe/+}$) mice at 60 hrs after hepatectomy were stained with Hematoxylin and Eosin (Magnification: 200x). Lipid droplets were shown by white droplets in the Hematoxylin and Eosin-stained tissue sections. PH, partial hepatectomy. (**B**) Levels of intracellular triglycerides in the livers of *Ire1α*-null and control mice under the non-stressed

condition or after 60 hrs of partial hepatectomy. Measurement of intracellular triglyceride levels was performed using a triglyceride assay kit according to manufacturer's instruction (BioAssay Systems, ETGA-200). ** $P<0.01$, n=3 mice per group.

Supplemental figure 8. A model depicting the role of IRE1α in maintaining hepatic lipid homeostasis.

References

Mitchell C, Willenbring H (2008) A reproducible and well-tolerated method for 2/3 partial hepatectomy in mice. *Nat Protoc* **3:** 1167-1170

Supplemental figure 1A

64 genes whose expression was decreased in the knockout (KO) liver (at least 1.5-fold decrease compared to that in the control (Ctl) liver, p<0.05)

		Ctl	KO	KO/Ctl	
Gene Symbol	**Genbank**	**N.A. value**	**N.A. value**	**Folds**	**Gene Description**
Snrpn	BB709603	1.106336	0.1591251	6.953	small nuclear ribonucleoprotein N
Tmepai	AV291712	1.256455	0.1946048	6.456	transmembrane, prostate androgen induced RNA
Xlr3a	NM_011726	0.883916	0.1382069	6.396	X-linked lymphocyte-regulated 3A
Pola2	AV326590	0.834934	0.1744544	4.786	polymerase (DNA directed), alpha 2
Arf4	BB754834	1.003703	0.2105785	4.766	ADP-ribosylation factor 4
Zfp312	NM_080433	0.596788	0.1560784	3.824	zinc finger protein 312
Syt6	AV165454	0.964552	0.2616363	3.687	synaptotagmin VI
Cyb561	BC006732	1.217992	0.34914	3.489	cytochrome b-561
Aff4	BB233318	0.850025	0.2504085	3.395	AF4/FMR2 family, member 4
Twist2	NM_007855	0.768495	0.2327472	3.302	twist homolog 2 (Drosophila)
Abi1	AW912678	0.457666	0.143734	3.184	abl-interactor 1
Lrrcc1	AK004646	1.040055	0.3363853	3.092	leucine rich repeat and coiled-coil domain containing 1
Dnajb5	AI664344	0.626192	0.2106713	2.972	DnaJ (Hsp40) homolog, subfamily B, member 5
Air	BB365661	1.482377	0.6372369	2.326	antisense Igf2r RNA
Slc1a4	BB277461	0.748341	0.3258698	2.296	solute carrier family 1, member 4
Rdh11	AB030503	1.864846	0.8584489	2.172	retinol dehydrogenase 11
Ccl9	AF128196	0.508151	0.2365402	2.148	chemokine (C-C motif) ligand 9
V2R2	NM_019918	0.892602	0.4267216	2.092	vomeronasal neurons putative pheromone receptor V2R2
LOC433755	AA189214	0.646608	0.3145227	2.056	hypothetical LOC433755
Mvd	NM_138656	0.830283	0.4144092	2.004	mevalonate (diphospho) decarboxylase
Crim1	BM234411	0.995102	0.5075338	1.961	Cysteine-rich repeat-containing protein CRIM1 (Crim1)
Trpm3	BB125842	1.006872	0.5174327	1.946	transient receptor potential cation channel, subfamily M, member 3
Cxadr	BE824924	0.673235	0.3464771	1.943	coxsackievirus and adenovirus receptor
Mvk	BC005606	2.504142	1.3035088	1.921	mevalonate kinase
Arrdc1	BC018501	1.312878	0.6950923	1.889	arrestin domain containing 1
Pstpip2	BC002123	1.312671	0.7104448	1.848	proline-serine-threonine phosphatase-interacting protein 2
Tlk2	AK014829	0.649527	0.3603371	1.803	tousled-like kinase 2 (Arabidopsis)
Dnajc3	BE624323	0.54686	0.3051605	1.792	DnaJ (Hsp40) homolog, subfamily C, member 3
Spcs2	BI078449	1.131494	0.645468	1.753	signal peptidase complex subunit 2 homolog
Nck1	BB296097	1.236411	0.7083386	1.746	non-catalytic region of tyrosine kinase adaptor protein 1
Tbl2	NM_013763	1.15668	0.666081	1.737	transducin (beta)-like 2
Sc4mol	AK005441	2.50624	1.4444478	1.735	sterol-C4-methyl oxidase-like
Acsl3	AK012088	1.310414	0.755519	1.734	acyl-CoA synthetase long-chain family member 3
Fdft1	NM_010191	1.928618	1.1140472	1.731	farnesyl diphosphate farnesyl transferase 1
Ssr4	NM_009279	1.220169	0.7124034	1.713	signal sequence receptor, delta
Smyd5	BF160651	0.687019	0.402269	1.708	SET and MYND domain containing 5
Dntt	AF316014	1.230267	0.7333166	1.678	deoxynucleotidyltransferase, terminal
Mall	BC012256	0.961877	0.5742328	1.675	mal, T-cell differentiation protein-like
Brwd3	BG066622	1.797896	1.077777	1.668	bromodomain and WD repeat domain containing 3
Gnpnat1	AK008566	0.759661	0.4595889	1.653	glucosamine-phosphate N-acetyltransferase 1

Pip5k1b	BB822856	0.706625	0.4305397	1.641	phosphatidylinositol-4-phosphate 5-kinase, type 1 beta
Letm1	BG060855	1.623128	0.9922701	1.636	leucine zipper-EF-hand containing transmembrane protein 1
Atf2	BM119623	0.951484	0.581706	1.636	activating transcription factor 2
Mknk1	AK010697	0.762839	0.4678569	1.63	MAP kinase-interacting serine/threonine kinase 1
Mvd	NM_138656	0.906597	0.556162	1.63	mevalonate (diphospho) decarboxylase
Tead1	BB546942	1.416145	0.8726368	1.623	TEA domain family member 1
Btg2	NM_007570	0.561845	0.3490928	1.609	B-cell translocation gene 2, anti-proliferative
Ythdf1	BB350365	1.183	0.738022	1.603	YTH domain family 1
Atp11c	AI593492	2.060446	1.2864633	1.602	Atpase, class VI, type 11C
Gorasp2	AK010664	1.160286	0.7266653	1.597	golgi reassembly stacking protein 2
Dnajb9	NM_013760	0.761702	0.4798189	1.587	DnaJ (Hsp40) homolog, subfamily B, member 9
Tmed3	NM_025360	0.711924	0.4486596	1.587	transmembrane emp24 domain containing 3
Mrgpre	BB373312	1.614723	1.0224634	1.579	MAS-related GPR, member E
Steap2	BB529332	1.576645	1.0122856	1.558	six transmembrane epithelial antigen of prostate 2
Gpr24	BE647763	1.959893	1.2711265	1.542	G protein coupled receptor 24
Nudcd1	AW542236	1.036232	0.6726758	1.54	NudC domain containing 1
H47	AK005204	0.669161	0.4350573	1.538	histocompatibility 47
Ropn1l	AF305427	1.983781	1.2916508	1.536	ropporin 1-like
Rnu22	BQ177137	0.328328	0.215546	1.523	RNA, U22 small nucleolar
Rnu22	BQ177137	0.316196	0.2075945	1.523	RNA, U22 small nucleolar
Gnal	BB306011	1.540748	1.0144672	1.519	guanine nucleotide binding protein, alpha stimulating, olfactory type
Ikbke	NM_019777	0.975424	0.6426376	1.518	inhibitor of kappaB kinase epsilon
Acss2	NM_019811	1.916789	1.2638172	1.517	acyl-CoA synthetase short-chain family member 2
Stch	BE650268	0.992851	0.6611507	1.502	stress 70 protein chaperone, microsome-associated, human homolog

N.A. value: normalized average exppression value

KO/Ctl: ratios of gene expression values of IRE1α null vs control.

Supplemental figure 1B

57 genes whose expression was increased in the knockout (KO) liver (at least 1.5-fold increase compared to that in the control (Ctl) liver, p<0.05)

		Ctl	KO	KO/Ctl	
Gene Symbol	**Genbank**	**N.A. value**	**N.A. value**	**Folds**	**Description**
Atp2a2	BG063183	0.515533	0.7786049	0.662	ATPase, Ca++ transporting, cardiac muscle, slow twitch 2
Cdon	BB125469	0.628787	0.9558229	0.658	Adhesion molecule-related/down-regulated by oncogenes
Rnu22	AW552536	0.412008	0.6265222	0.658	RNA, U22 small nucleolar
Gm967	AW457804	0.54835	0.8395036	0.653	gene model 967, (NCBI)
Ddit3	NM_007837	0.028109	0.0433388	0.649	DNA-damage inducible transcript 3
Zfp207	AI646720	0.37787	0.5858806	0.645	Zinc finger protein 207, mRNA
Nfasc	BB409198	0.989849	1.5413092	0.642	neurofascin
Cad	AK010453	0.334711	0.5245007	0.638	carbamoyl-phosphate synthetase 2
Zfp592	BB478535	0.619713	0.9814639	0.631	zinc finger protein 592
4930432B04Rik	BB437636	0.673198	1.0686985	0.63	Cytoskeleton associated protein 5, mRNA
Rapgef2	BM120546	0.513634	0.8223091	0.625	Rap guanine nucleotide exchange factor (GEF) 2, mRNA
Pbx3	BB554874	0.575067	0.9251468	0.622	pre B-cell leukemia transcription factor 3
Nedd4l	BB360028	0.25571	0.4139056	0.618	Neural cell developmentally down-regulated gene 4-like
Apoa5	AA254866	1.401669	2.2762778	0.616	Apolipoprotein A-V (Apoa5), mRNA
Rab2b	AK005230	0.506506	0.8229689	0.615	RAB2B, member RAS oncogene family
Mpp4	AB059357	1.238018	2.0285037	0.61	membrane protein, palmitoylated 4
Phr1	BM238052	0.589302	0.9722936	0.606	Pam, highwire, rpm 1 (Phr1), mRNA
Mettl4	BB701076	0.506154	0.8473486	0.597	methyltransferase like 4
Dock4	BB656539	1.514044	2.5413232	0.596	dedicator of cytokinesis 4
Phip	BM218981	1.295397	2.1799352	0.594	pleckstrin homology domain interacting protein
Kctd13	BQ177107	0.543341	0.9328961	0.582	potassium channel tetramerisation domain containing 13
Pkp2	AK004731	0.513869	0.8937289	0.575	plakophilin 2
Hist1h1c	BB533903	0.315064	0.5486828	0.574	histone 1, H1c
Bach2	BI104953	1.052494	1.8663629	0.564	BTB and CNC homology 2 (Bach2), mRNA
Arfrp2	AI785253	0.434556	0.7710369	0.564	ADP-ribosylation factor related protein 2 (Arfrp2), mRNA
Gle1l	AV228343	0.422612	0.7501699	0.563	GLE1 RNA export mediator-like
Derl3	AK007348	0.019531	0.0357669	0.546	Der1-like domain family, member 3
Mdm1	AV313203	0.365482	0.6745294	0.542	transformed mouse 3T3 cell double minute 1
Bcl7c	BB176719	0.964105	1.8177955	0.53	B-cell CLL/lymphoma 7C
Yipf4	AV216410	0.507096	0.9613949	0.527	Yip1 domain family, member 4
Eif3s6ip	AV216873	0.648856	1.2522556	0.518	translation initiation factor 3, subunit 6 interacting protein
Tnfrsf9	BC028507	0.611113	1.1897492	0.514	tumor necrosis factor receptor superfamily, member 9
Arfrp2	BM214060	0.427078	0.8488674	0.503	ADP-ribosylation factor related protein 2 (Arfrp2), mRNA
Nedd4l	BB309512	0.321554	0.64352	0.5	neural cell developmentally down-regulated gene 4-like
Ddit3	BB200603	0.349908	0.7010221	0.499	DNA-damage inducible transcript 3
Nr4a2	NM_013613	0.468023	0.9377375	0.499	nuclear receptor subfamily 4, group A, member 2
Mnab	BM210927	0.471156	0.9532796	0.494	membrane associated DNA binding protein
Col9a3	BG074456	0.775138	1.606882	0.482	procollagen, type IX, alpha 3
Phf6	BF147362	0.449741	0.9673274	0.465	PHD finger protein 6
Cdkn1a	AK007630	0.085497	0.1869583	0.457	cyclin-dependent kinase inhibitor 1A (P21)

Ddit4	AK017926	0.262658	0.5748734	0.457	DNA-damage-inducible transcript 4
Psat1	BC004827	0.012318	0.0273046	0.451	phosphoserine aminotransferase 1
Susd4	BF455403	1.061193	2.371801	0.447	sushi domain containing 4
Tktl1	C79967	0.777513	1.8779701	0.414	Transketolase-like 1 (Tktl1), mRNA
Phox2a	NM_008887	0.347061	0.8547047	0.406	paired-like homeobox 2a
Styk1	AV375472	0.228523	0.5910682	0.387	serine/threonine/tyrosine kinase 1
Esrrg	BM120183	0.663688	1.7384369	0.382	estrogen-related receptor gamma
Scara5	BC016096	0.888253	2.352793	0.378	scavenger receptor class A, member 5 (putative)
Mrvi1	U63408	0.38448	1.1671803	0.329	MRV integration site 1
Ddx50	AA518255	0.140597	0.4892876	0.287	DEAD (Asp-Glu-Ala-Asp) box polypeptide 50
H1fx	BI416101	0.128748	0.4861345	0.265	H1 histone family, member X
Bicc1	BB497148	0.161315	0.6333181	0.255	Bicaudal C homolog 1 (Drosophila) (Bicc1), mRNA
Asns	BC005552	0.121902	0.5628594	0.217	asparagine synthetase
Trpc1	BB817939	0.176141	1.1086509	0.159	transient receptor cation channel, subfamily C, member 1
Mrc2	AW555385	0.132763	0.9969737	0.133	Mannose receptor, C type 2 (Mrc2), mRNA
Asns	AV212753	0.066149	0.5234336	0.126	asparagine synthetase
Atad1	AV017609	0.130715	1.0529606	0.124	ATPase family, AAA domain containing 1

N.A. value: normalized average exppression value

KO/Ctl: ratios of gene expression values of IRE1α null vs control.

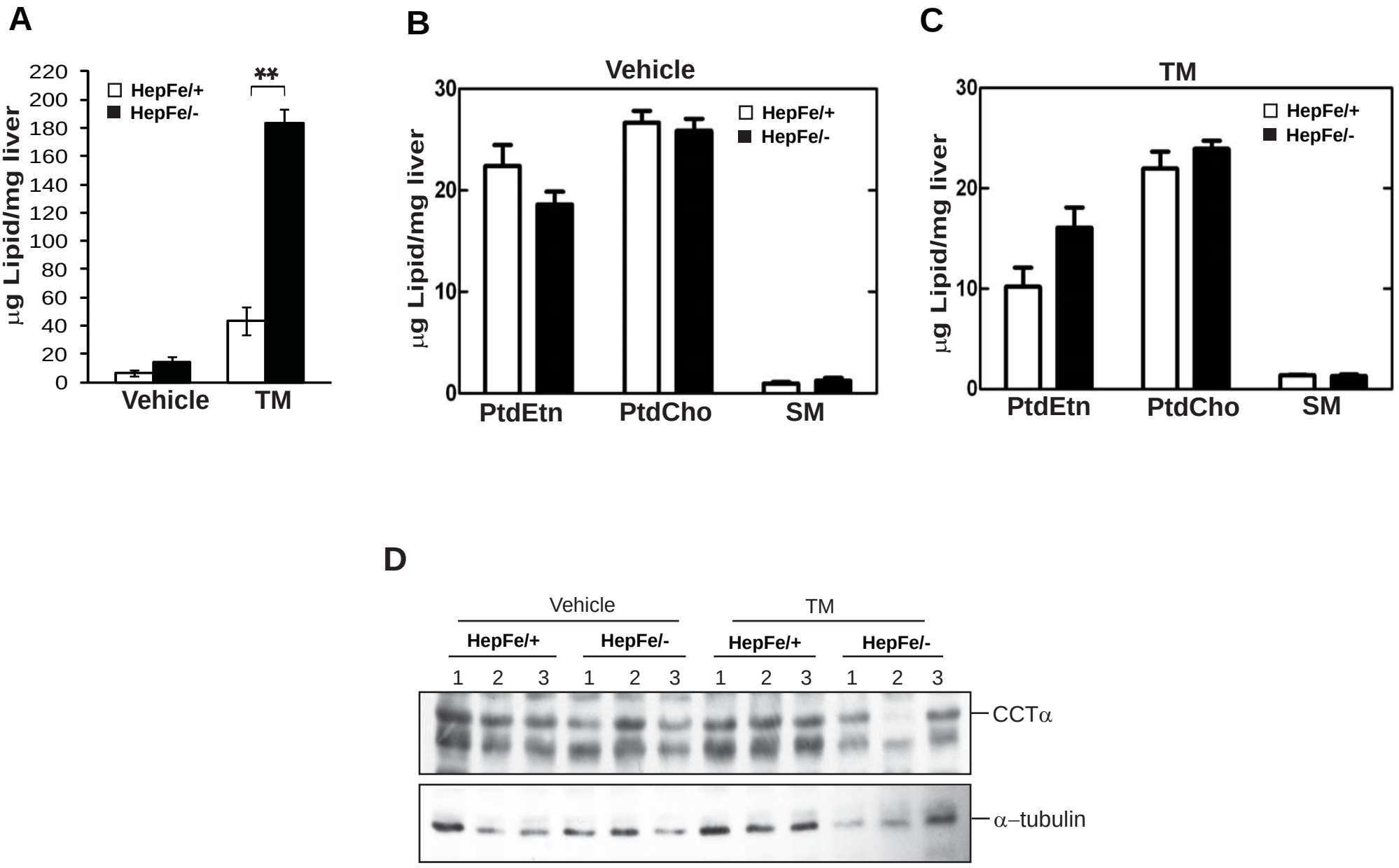

Supplemental figure 2

A

Threshold cycle

	PPARgamma2				beta-actin			
	Liver		White adipose		Liver		White adipose	
mice ID#	Chow Diet	High Fat Diet	Chow Diet	High Fat Diet	Chow Diet	High Fat Diet	Chow Diet	High Fat Diet
1	33.12	29.03	25.38	29.20	19.30	18.75	15.47	16.20
2	34.95	28.38	24.37	25.32	20.64	19.34	16.19	14.81
3	32.82	28.43	25.32	24.82	20.73	19.36	15.70	14.67
4	N/A	30.73	27.35	26.96	19.30	19.75	15.78	15.32
5	N/A	28.01	27.68	25.41	19.03	19.03	15.66	15.30

	PPARgamma2				beta-actin			
	wild-type		IRE-KO		wild-type		IRE-KO	
mice ID#	saline	tunicamycin	saline	tunicamycin	saline	tunicamycin	saline	tunicamycin
1	33.07	32.38	33.34	31.42	15.70	14.84	14.66	15.71
2	31.89	32.97	33.33	N/A	15.02	14.84	15.70	15.41
3	31.99	31.97	N/A	32.02	15.27	15.61	15.30	14.11

B

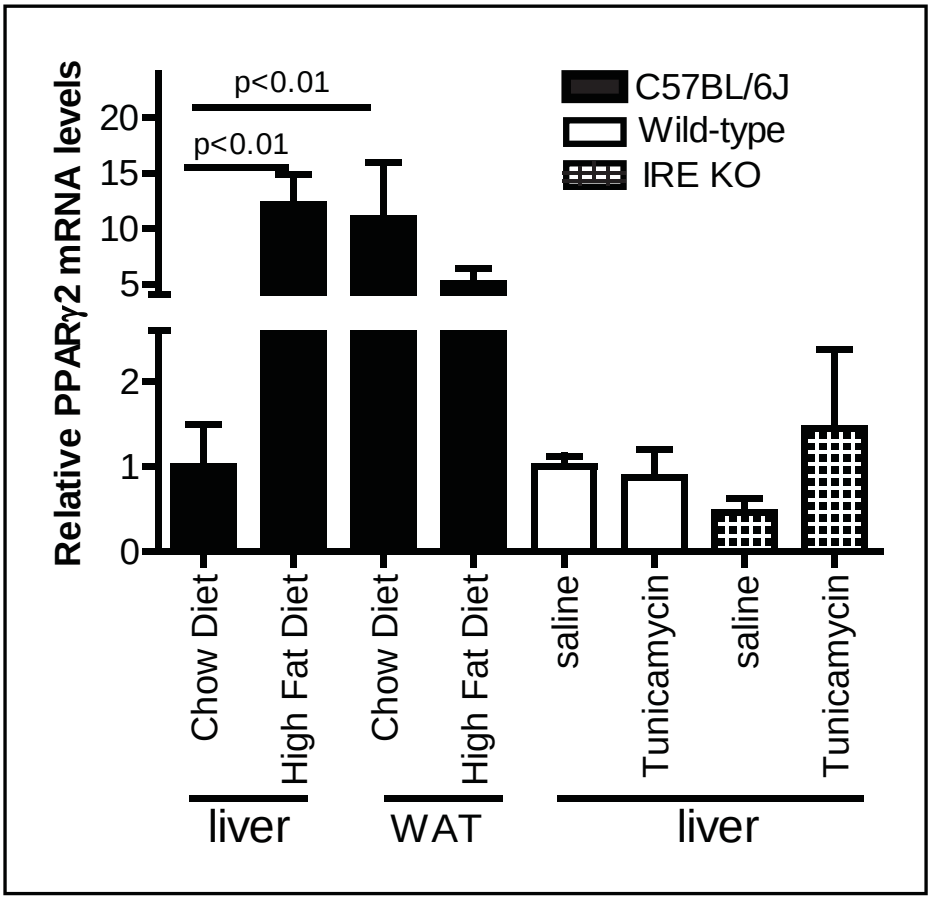

Supplemental figure 3

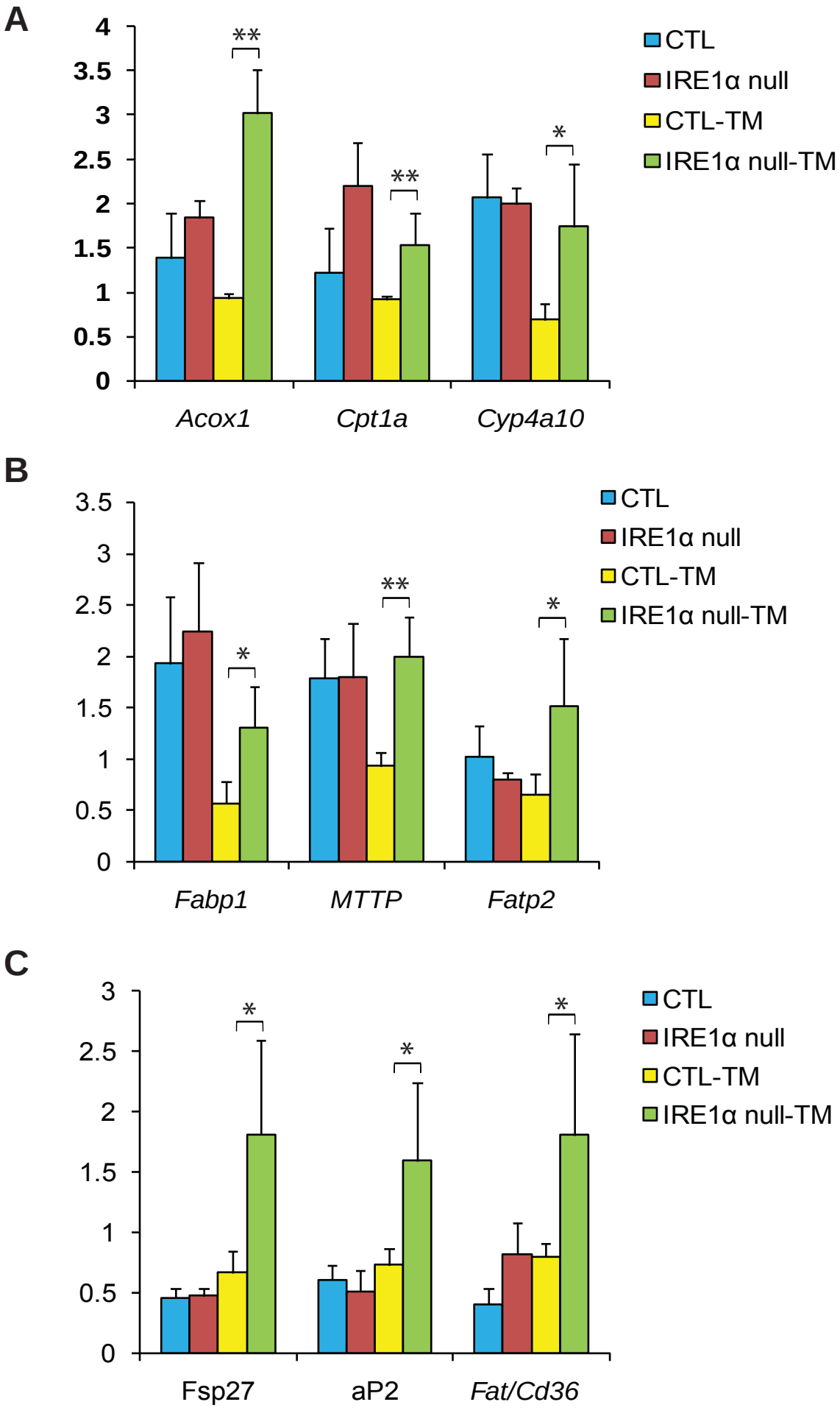

Supplemental figure 4

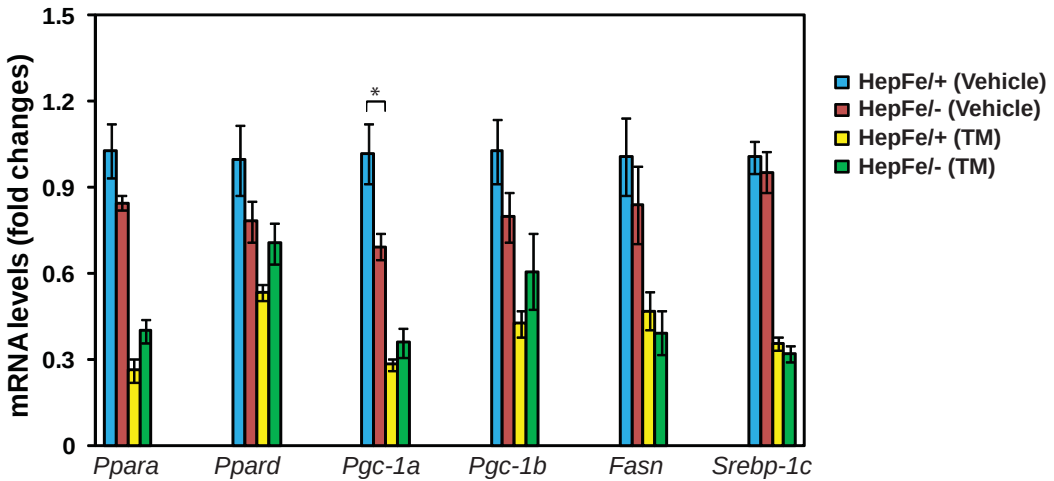

Supplemental figure 5

A

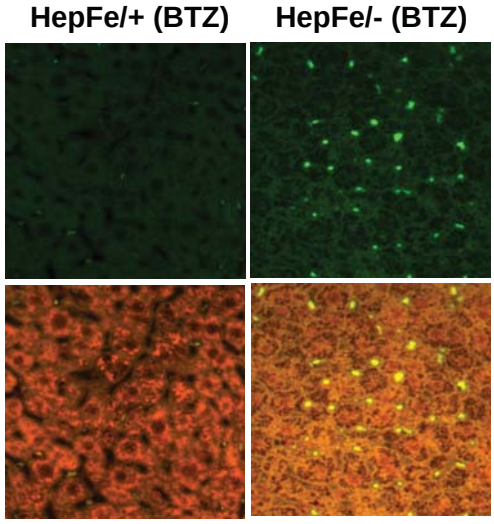

B

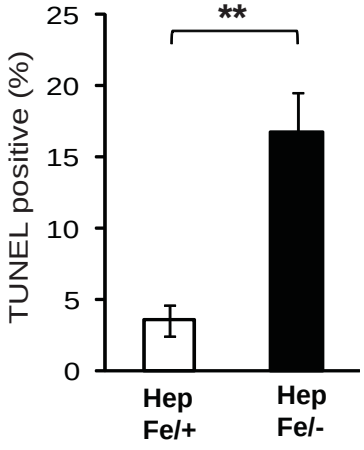

Supplemental figure 6

A

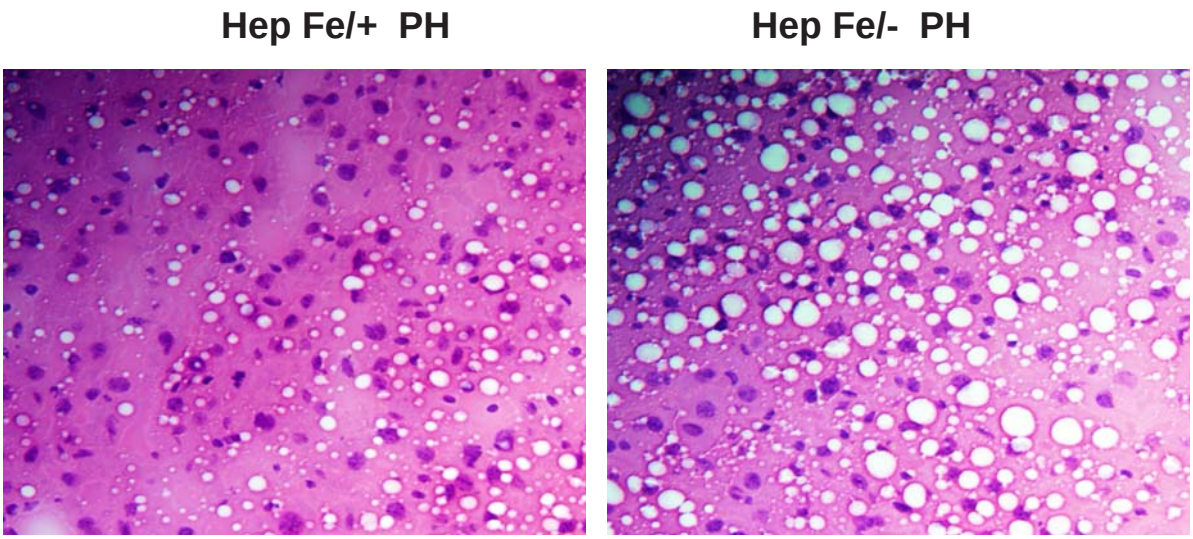

B

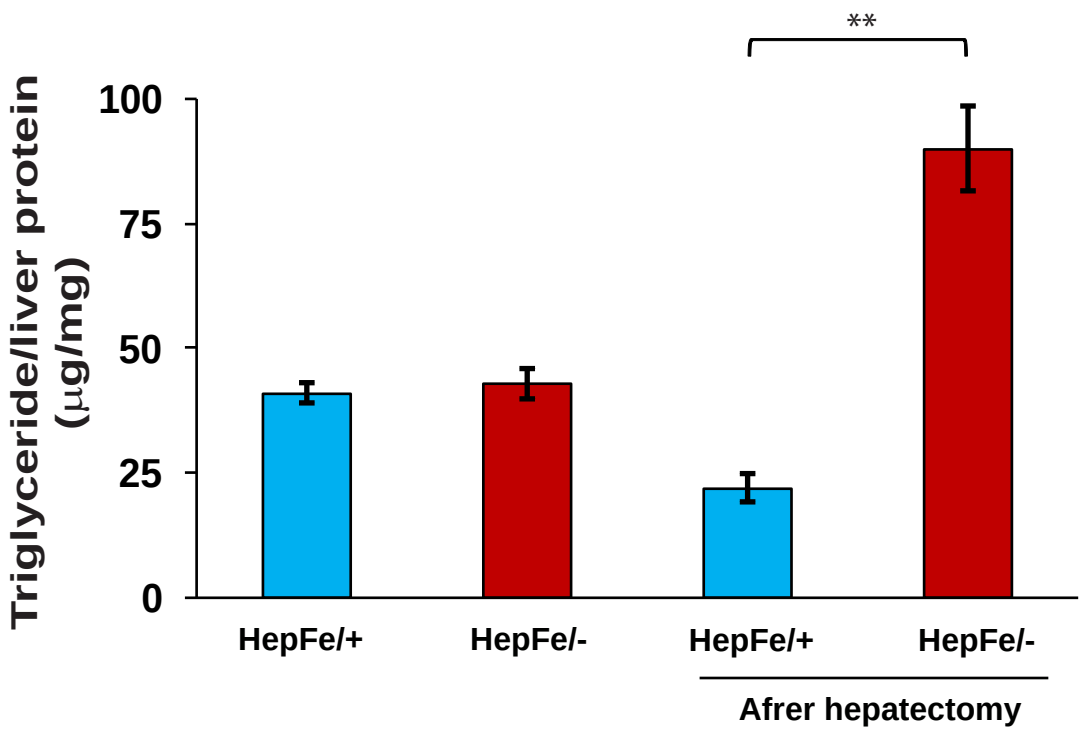

Supplemental figure 7

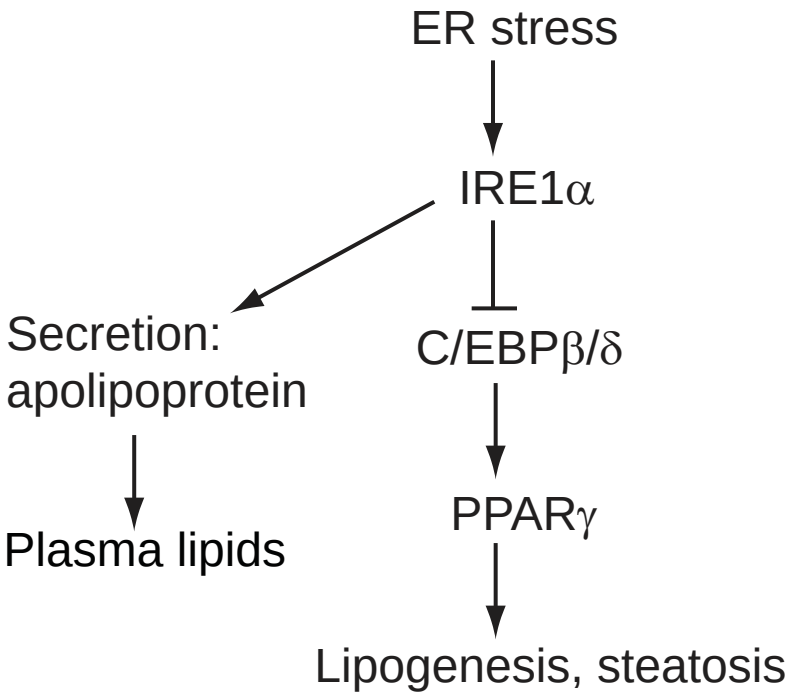

Supplemental figure 8